Left-Handed Helical Ribbon Intermediates in the Self-Assembly of a β-Sheet Peptide

Davide M. Marini,[†] Wonmuk Hwang,[‡] Douglas A. Lauffenburger,[§] Shuguang Zhang,*,[‡] and Roger D. Kamm*,[†,§]

Department of Mechanical Engineering, Center for Biomedical Engineering, and Division of Bioengineering and Environmental Health, Massachusetts Institute of Technology, 77 Massachusetts Avenue, Cambridge, Massachusetts 02139-4307

ABSTRACT

We report the observation of intermediate structures in the self-assembly of the peptide KFE8 (FKFEFKFE), designed with alternating polar and nonpolar amino acids. Self-assembly was followed over time using atomic force microscopy (AFM), transmission electron microscopy (TEM), and circular dichroism (CD). Molecular dynamics simulations suggest that these intermediates are left-handed double helical β-sheets. These findings have implications in the study of β-sheet fibril formation, and in the molecular design of materials.

Molecular self-assembly has attracted considerable attention as a means of creating designed materials and devices for nanotechnology.[1–6] One of the most ubiquitous self-assembly processes in nature is the hierarchical organization of protein monomers into long filaments, bundles, and networks. Following the repetitive patterns found in the sequence of natural fibrous proteins (such as silk fibroin, collagen, and spider silk), we have designed short peptides using an alternating pattern of hydrophobic–hydrophilic amino acids.[7] Aqueous solutions of these peptides form hydrogels under appropriate ionic strength or pH;[8] at the microscopic level, they appear as networks of nanometer-scale fibers and are currently used as scaffolds for three-dimensional cell culture.[9] To deepen our understanding of this self-assembly process and to eventually be able to design fibers and other structures of pre-specified properties, we followed the self-assembly of KFE8 over time and characterized its intermediate configurations.

Our previous studies[7,8] showed that self-assembly of KFE8 is extremely rapid when either of the following conditions is met: (a) the ionic strength of the solution is above a certain threshold, or (b) its pH is such that the net charge on the molecule is almost zero. Yet, to capture the intermediate steps of self-assembly, it is necessary to decrease the speed of this process. We therefore dissolved the peptide in deionized water and the pH of the solution (~3.3) was such that KFE8 molecules were mostly positively charged. Such a condition

considerably reduced the speed of self-assembly, making it possible to visualize its intermediate structures.

AFM images collected a few minutes after preparation of the peptide solution revealed the presence of left-handed helical ribbons (Figure 1a) of pitch 19.1 ± 1.2 nm. Such structures were also observed after deposition of the solution on substrates other than mica (graphite and silicon, data not shown). Electron microscopy performed on quick-frozen aliquots taken from solution confirmed the structure and chirality of these helical ribbons (Figure 1a, inset). These observations suggest that helical ribbons are formed in water and are not a result of interaction between KFE8 and the substrate. The diameter of these helices was computed from their pitch and pitch angle (assuming cylindrical geometry) as 7.1 ± 1.1 nm. The average length of helical ribbons remained approximately constant at ~90 nm until they disappeared after ~2 h (Figure 1c). A second type of fibrillar structure of ~8 nm diameter appeared with increasing frequency at later stages and further assembled into bands of parallel filaments (Figure 1d) forming a network.

Self-assembly of KFE8 was also monitored over time with CD. One minute after dissolving the peptide in water, the CD spectrum was characterized by a typical β-sheet profile. Spectra collected over time indicated a steady increase in antiparallel β-sheet structures and a concurrent decrease in the presence of random coils.

The prevalence of helical ribbons at early stages and their subsequent disappearance suggests that they are intermediates in the formation of fibers (a phenomenon observed at a larger

---

* To whom correspondence should be addressed. E-mail: shuguang@mit.edu, rdkamm@mit.edu.
† Department of Mechanical Engineering.
‡ Center for Biomedical Engineering.
§ Division of Bioengineering and Environmental Health.
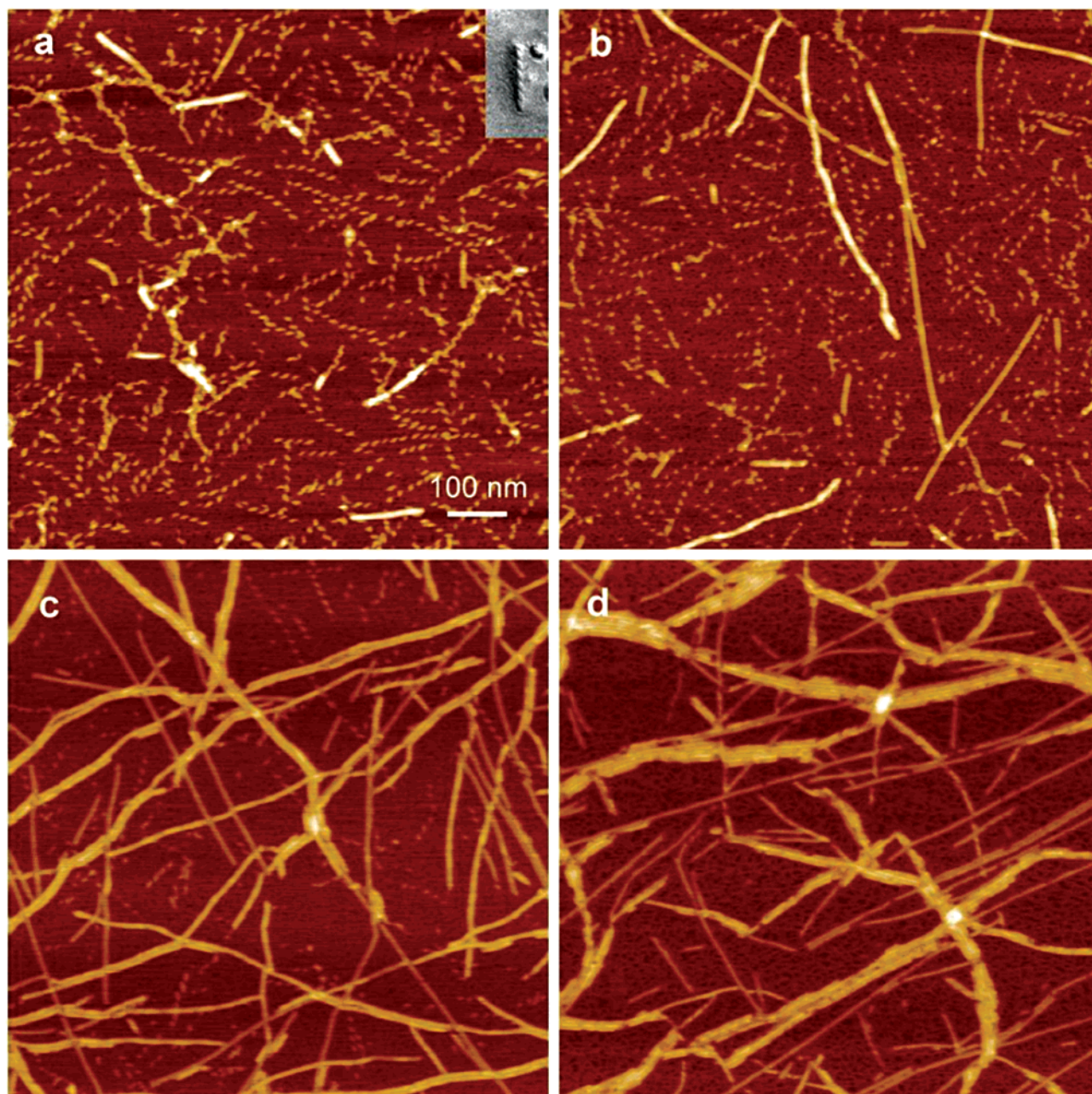
Figure 1. Intermediate structures in the self-assembly of KFE8 in aqueous solution. Images are AFM scans (the brightness of features increases as a function of height) of a freshly cleaved mica surface over which aliquots taken from solution were deposited at different times after preparation of the solution. **a**, after 8 min. Inset: electron micrograph of a sample of peptide solution obtained using the quick-freeze deep-etch technique. **b**, 35 min after preparation. **c**, 2 h. **d**, 30 h.
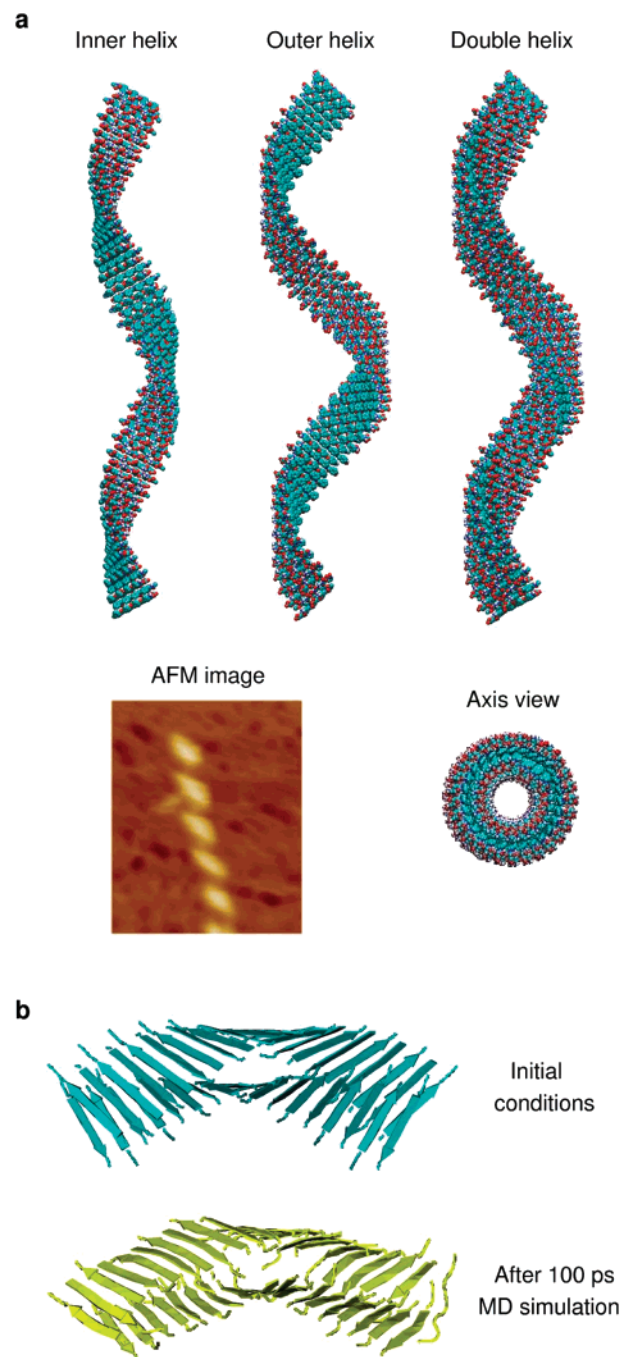
length scale in lipids[10,11] and chlorophenols[12]). To control this self-assembly process, it is important to characterize the molecular architecture of these intermediates and ultimately the dynamics of their formation. In this study we investigated their structure using molecular dynamics simulation. Our CD measurements indicate that KFE8 molecules organize in solution into β-sheet structures; similar peptides, derived from segments of native proteins, have also been shown to assemble into β-sheet tapes in suitable solvents.[13,14] Therefore, we constructed and tested the stability of various β-sheet configurations by checking the distortion of their geometry and the preservation of β-sheet content during molecular dynamics. Preliminary simulations showed that the parallel

β-sheet conformation is less stable than the antiparallel, in agreement with our CD results. Thus, we focused on antiparallel β-sheets, which, due to the asymmetric distribution of backbone hydrogens and oxygens of KFE8 (Figure 2a), limit the number of hydrogen bonding patterns with adjacent molecules to two on each side (Figure 2b). Therefore, a total of four different antiparallel β-sheet conformations is possible (Figure 2c). Using all the combinations of these four types of sheets, we constructed single and double helical ribbons of 20 nm pitch and 7 nm diameter (Figure 3a). Molecular dynamics simulation was then performed on these structures to test their stability in water. Single-sheet helices were found to be unstable, collapsing im-
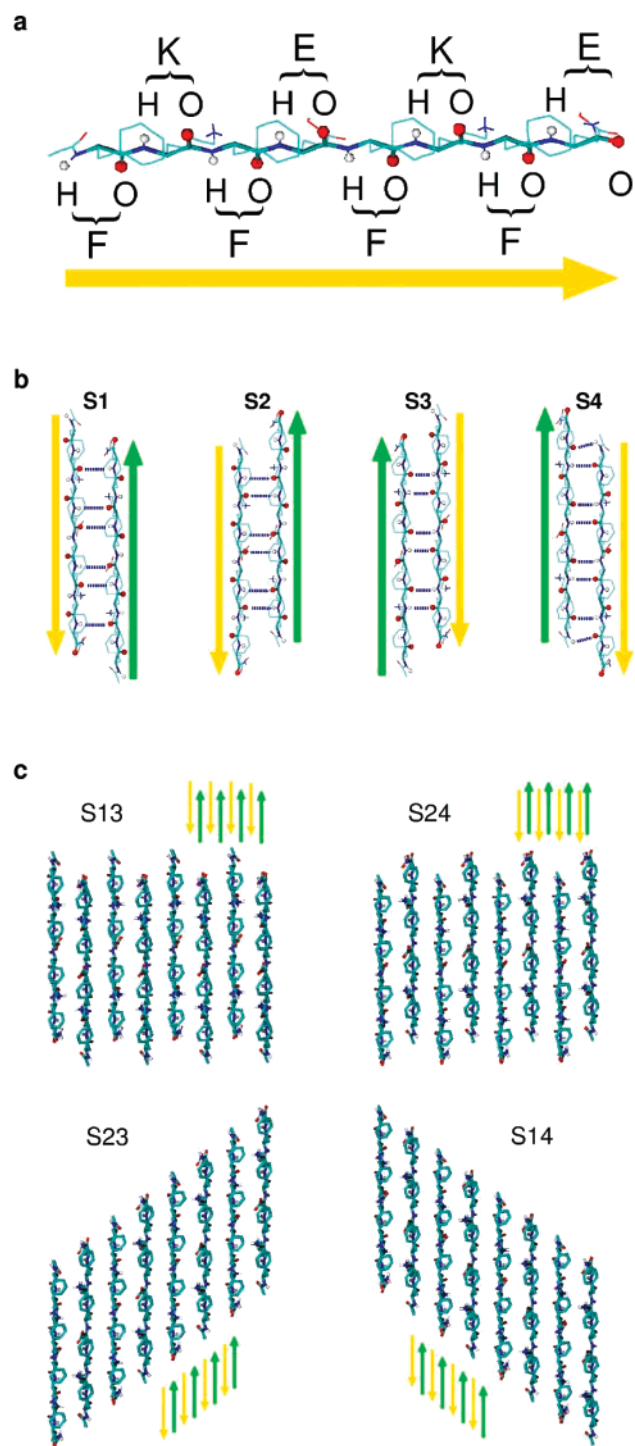
Figure 2. Hierarchical construction of possible β-sheets. **a**, Asymmetry in the distribution of KFE8 backbone hydrogens and oxygens. **b**, Possible hydrogen bond patterns between two peptides. S1 and S2 are the possible hydrogen bonds on the right-hand side of the peptide represented by the yellow arrow (phenyl rings are facing the reader). Similarly, S3 and S4 are the possible bonds on its left-hand side. **c**, Four β-sheets constructed using the paired configurations in (b). Sij represents the combination of Si ($i = 1,2$) and Sj ($j = 3,4$) connections.

Figure 3. Molecular modeling and simulation of a left-handed double helical β-sheet. **a**, Construction of a double helix. The S13 and S24 sheets are respectively used for the inner and outer sheets. Hydrophobic side chains are buried between the two helices. One helical turn is 20 nm and the diameter is 7 nm. **b**, Side view of the segment of double helix used in simulations. Above: Initial configuration. Below: result after 100 ps of molecular dynamics.

mediately, because the hydrophobic side of the β-sheet was still exposed to the solvent. Double helical β-sheets with the S13 sheet on the inside and either the S13 or the S24 sheet on the outside (Figure 3a) were found to be the most stable structures (Figure 3b, more detailed simulation results will be published elsewhere). Maintaining the same supramolecular architecture, we then investigated its sensitivity to helical pitch. We tested 15 and 25 nm pitches and found them to be less stable than helices with a 20 nm pitch. We are currently investigating the possibility that the helix-to-fiber transition may be the result of tighter coiling of these intermediate helical ribbons.[11]

The tendency of KFE8 to form regular structures makes this molecule a very attractive model system for studying the self-assembly of protein fibrils. Its small size allows one to easily modify the sequence and test the resulting structures both experimentally and numerically. Such an approach will help in the rational design of biological materials and other nanoscale devices. Furthermore, the fibers formed by KFE8 bear the same chirality[15,16] and have dimensional similarities with a broad range of amyloid fibers.[17-21] This is probably because amyloid fibrils are formed by certain segments of partially unfolded proteins that assemble into β-sheets.[18,22] We believe the self-assembly of KFE8 is a simplified version of this process and our observation of the intermediates can provide important insights into its dynamics.

Experimental Methods. *Peptide Synthesis and Sample Preparation.* The peptide KFE8, of sequence $[COCH_3]-$ FKFEFKFE$-[CONH_2]$, was custom-synthesized from Research Genetics, Inc. (Huntsville, AL) and the lyophilized powder was stored at 4 °C. Solutions of KFE8 were prepared by mixing the powder with deionized water and vortexing for 1 min. The solution was stored at room temperature and showed no visible precipitate even after months. The typical concentration was 1 mg/mL (0.86 mM) and the pH was ~3.3.

AFM. Aliquots of $4-8\ \mu L$ were removed from the peptide solution at various times after preparation and deposited onto a freshly cleaved mica surface. To optimize the amount of peptide adsorbed, each aliquot was left on mica for $10-30$ s and then rinsed with $50-100\ \mu L$ of deionized water (rinsing with water adjusted at pH ~3.3 with HCl did not change the results). The mica surface with the adsorbed peptide was then dried in air and imaged immediately. The images shown were obtained by scanning the mica surface in air by AFM (Multimode, Digital Instruments, Santa Barbara, CA) operating in Tapping Mode. Deposition of the peptide solution onto a different substrate (hydrophobic graphite and silicon) followed by AFM imaging revealed essentially the same fiber structures (data not shown). When imaging soft biopolymers with AFM at high resolution, it is important to minimize the tip tapping force. Soft silicon cantilevers were chosen (FESP model, Digital Instruments, Santa Barbara, CA) with spring constant of $1-5$ N/m and tip radius of curvature of $5-10$ nm. AFM scans were taken at 512×512 pixels resolution and produced topographic images of the samples, in which the brightness of features increases as a function of height. Typical scanning parameters were as follows: tapping frequency ~70 kHz, RMS amplitude before engage $1-1.2$ V, integral and proportional gains $0.2-0.6$ and $0.3-1$ respectively, setpoint $0.8-1$ V, scanning speed $1-2$ Hz.

TEM. Aliquots of ~5 μL were taken from peptide solution, deposited over a gold sample holder and quick-frozen in liquid propane. The frozen droplets were deep-etched for 36 min at -100 °C and the exposed structures were rotary-replicated with a layer of ~1.5 nm of platinum and ~20 nm of carbon. Replicas were removed in a sodium hypochlorite bath (Clorox brand), picked up on microscope grids and viewed under a Philips-300 transmission electron microscope (Eindhoven, The Netherlands).

CD. The peptide solution was injected immediately after preparation into a quartz cuvette with a path length of 0.1 cm. CD spectra were recorded (AVIV model 202) at several times between 1 and 200 min after preparation, in the wavelength range $190-240$ nm. The wavelength step was 1 nm and the averaging time was 1 s. Secondary structure fractions were deduced from the spectra using the software CDNN 2.1.[23]

Numerical Simulations. Individual KFE8 molecules were built using the extended atom representation of CHARMM[24] with parameter set version 19. Solvent (water) was modeled through the analytic continuum electrostatics (ACE) module.[25] Four single helices and sixteen double helices were constructed, comprised of combinations of the β-sheets in Figure 2c (for example, Figure 3a). For the simulation of double helices, 40 KFE8 molecules were used to construct a segment of the helix, comprising about 40% of a full helical turn. Molecular dynamics simulations were performed in stages: 20 ps of heating, 20 ps of equilibration and 100 ps of production run at 300 K. Coordinates during the production run were averaged and further energy minimized to obtain the final structures as in Figure 3b.

References

(1) Stupp, S. I.; LeBonheur, V.; Walker, K.; Li, S. L.; Huggins, K. E.; Keser, M.; Amstutz, A. *Science* **1997**, *276*, 384−389.
(2) Muthukumar, M.; Ober, C. K.; Thomas, E. L. *Science* **1997**, *277*, 1225−1232.
(3) Petka, W. A.; Harden, J. L.; McGrath, K. P.; Wirtz, D.; Tirrell, D. A. *Science* **1998**, *281*, 389−392.
(4) Breen, T. L.; Tien, J.; Oliver, S. R. J.; Hadzic, T.; Whitesides G. M. *Science* **1999**, *284*, 948−951.
(5) Orr, G. W.; Barbour, L. J.; Atwood, J. L. *Science* **1999**, *285*, 1049−1052.
(6) Dubois, M.; Deme, B.; Gulik-Krzywicki, T.; Dedieu, J. C.; Vautrin, C.; Desert, S.; Perez, E.; Zemb, T. *Nature* **2001**, *411*, 672−675.
(7) Zhang, S.; Holmes, T.; Lockshin, C.; Rich, A. *Proc. Natl. Acad. Sci. U.S.A.* **1993**, *90*, 3334−3338.
(8) Caplan, M. R.; Moore, P. N.; Zhang, S.; Kamm, R. D.; Lauffenburger, D. A. *Biomacromolecules* **2000**, *1*, 627−631.
(9) Holmes, T. C.; de Lacalle, S.; Su, X.; Liu, G.; Rich, A.; Zhang, S. *Proc. Natl. Acad. Sci. U.S.A.* **2000**, *97*, 6728−6733.
(10) Schnur, J. M.; Ratna, B. R.; Selinger, J. V.; Singh, A.; Jyothi, G.; Easwaran, K. R. K. *Science* **1994**, *264*, 945−947.
(11) Zastavker, Y. V.; Asherie, N.; Lomakin, A.; Pande, J.; Donovan, J. M.; Schnur, J. M.; Benedek, G. *Proc. Natl. Acad. Sci. U.S.A.* **1999**, *96*, 7883−7887.
(12) Rogalska, E.; Rogalski, M.; Gulik-Krzywicki, T.; Gulik, A.; Chipot, C. *Proc. Natl. Acad. Sci. U.S.A.* **1999**, *96*, 6577−6580.
(13) Aggeli, A.; Bell, M.; Boden, N.; Keen, J. N.; Knowles, P. F.; McLeish, T. C. B.; Pitkealthy, M.; Radford, S. E. *Nature* **1997**, *386*, 259−262.
(14) Aggeli, A.; Nyrkova, I. A.; Bell, M.; Harding, R.; Carrick, L.; McLeish, T. C. B.; Semenov, A. N.; Boden, N. *Proc. Natl. Acad. Sci. U.S.A.* **2001**, *98*, 11 857−11 862.

(15) Shamovsky, I. L.; Ross, G. M.; Riopelle, R. J. *J. Phys. Chem. B* **2000**, *104*, 11 296−11 307.

(16) Chamberlain, A. K.; MacPhee, C. E.; Zurdo, J.; Morozova-Roche, L. A.; Hill, H. A. O.; Dobson, C. M.; Davis, J. J. *Biophys. J.* **2000**, *79*, 3283−3293.

(17) Harper, J. D.; Wong, S. S.; Lieber, C. M.; Lansbury, P. T. Jr. *Biochemistry* **1999**, *38*, 8972−8980.

(18) Balbirnie, M.; Grothe, R.; Eisenberg, D. S. *Proc. Natl. Acad. Sci. U.S.A.* **2001**, *98*, 375−2380.

(19) Kowalewski, T.; Holtzman, D. M. *Proc. Natl. Acad. Sci. U.S.A.* **1999**, *96*, 3688−3693.

(20) Choo, D. W.; Schneider, J. P.; Graciani, N. R.; Kelly, J. W. *Macromolecules* **1996**, *29*, 355−366.

(21) Koo, E. H.; Lansbury, P. T. Jr.; Kelly, J. W. *Proc. Natl. Acad. Sci. U.S.A.* **1999**, *96*, 9989−9990.

(22) Dobson, C. M. *Philos T Roy Soc B* **2001**, *356*, 133−145.

(23) Bohm, G.; Muhr, R.; Jaenicke, R. *Protein Eng.* **1992**, *5*, 191−195.

(24) Brooks, B. R.; Bruccoleri, R. E.; Olafson, B. D.; States, D. J.; Swaminathan, S.; Karplus, M. *J. Comput. Chem.* **1983**, *4*, 187−217.

(25) Schaefer, M.; Karplus, M. *J. Phys. Chem.* **1996**, *100*, 1578−1599.

NL015697G